Available online at www.sciencedirect.com
ScienceDirect
Applied Catalysis B: Environmental 83 (2008) 96–109
APPLIED CATALYSIS B: ENVIRONMENTAL
www.elsevier.com/locate/apcatb

Testing in annular micro-reactor and characterization of supported Rh nanoparticles for the catalytic partial oxidation of methane: Effect of the preparation procedure

Alessandra Beretta [a,*], Alessandro Donazzi [a], Gianpiero Groppi [a], Pio Forzatti [a], Vladimiro Dal Santo [b], Laura Sordelli [b], Valentina De Grandi [c], Rinaldo Psaro [b]

[a] *Laboratorio di Catalisi e Processi Catalitici, Dipartimento di Energia, Politecnico di Milano, piazza Leonardo da Vinci 32, 20133 Milano, Italy*
[b] *ISTM-CNR via Golgi 19, 20133 Milano, Italy*
[c] *Dipartimento CIMA Università degli Studi di Milano, via Venezian 21, 20133 Milano, Italy*

Received 19 December 2007; received in revised form 5 February 2008; accepted 9 February 2008
Available online 15 February 2008

Abstract

This work extends a previous study on the conditioning of Rh/Al_2O_3 during CH_4-CPO experiments at high space velocity. The effect of the preparation procedure was investigated by comparing well-known preparation techniques such as incipient wetness impregnation and grafting, and a novel CVD technique. Catalysts prepared by impregnation of the support with a solution of $Rh(NO_3)_3$ showed a very slow activation process, starting from an initially poor syngas activity and ending up to outstanding performances. Catalysts prepared by grafting of $Rh_4(CO)_{12}$ onto alumina showed a similar behaviour, but the initial activity was closer to final activity (similarly high). Catalysts prepared by CVD of $Rh(acac)(CO)_2$ showed very good and stable performances from the very initial CPO run. To better understand the morphological changes which occur during reaction conditions, H_2 chemisorption, CO chemisorption, CO-DRIFT and HRTEM were applied in concert to analyze the surface of samples prior and after catalytic testing. Characterization results support the hypothesis that the conditioning process is related to a reconstruction of the Rh particles which tends to eliminate small defective clusters and particles, wherein C-forming reactions are presumably highly favoured. The extent of reconstruction is thus strictly related to the heterogeneity of the surface, which is affected by the preparation procedure; heterogeneity is high over samples prepared *via* impregnation and grafting, low over sample prepared by CVD.

Keywords: Rh nanoparticles; Catalytic partial oxidation of CH_4; CVD; HRTEM; CO-DRIFTS; H_2 chemisorption; CO chemisorption

1. Introduction

In previous studies we have reported that highly dispersed $Rh/\alpha\text{-}Al_2O_3$ catalysts at low Rh loads undergo an activation process during repeated CH_4 partial oxidation runs, with progressive enhancement of the syngas yield in the temperature range 500–850 °C. The conditioning proceeds until reaching of extremely high performances, close to thermodynamic equilibrium, even operating at few ms contact times [1,2]. Several studies suggest that CH_4 partial oxidation over Rh and other metals (that is the combined activation of CH_4 by O_2, H_2O and CO_2) involves a network of structure sensitive reaction steps (including C–H and C–O bonds breaking) [3–7], so that the observed activation was interpreted as the chemical effect of a surface reconstruction (with loss of defects), driven by the high reaction temperature and the adsorption of gas-phase species. Indeed, changes of the surface Rh species were observed by FT-IR on $Rh/\alpha\text{-}Al_2O_3$ and Rh/ZrO_2 catalysts after treatments in several gaseous mixtures, representative of the CPO reaction process [8].

In this work, the research was extended and efforts were spent to better comprehend the nature of the Rh species on highly dispersed systems and the effect of their changes on the syngas catalysis.

$Rh/\alpha\text{-}Al_2O_3$ catalysts obtained by different preparation procedures, including incipient wetness impregnation, grafting and chemical vapor deposition, were analyzed. The adopted methodologies were expected to produce different interactions

* Corresponding author.
E-mail address: alessandra.beretta@polimi.it (A. Beretta).

0926-3373/$ – see front matter © 2008 Elsevier B.V. All rights reserved.
doi:10.1016/j.apcatb.2008.02.007

with the support and consequently different particle distributions. The study consisted of a comparative analysis of the catalytic performance (during conditioning and at steady-state) and of the surface properties of the different materials. CH_4-CPO experiments were performed in an annular wall reactor at high space velocity, under kinetically controlled conditions which enable to investigate the initial reaction transients. HRTEM, IR-spectroscopy, chemisorption of H_2 and CO, well established techniques for the characterization of highly dispersed Rh-catalysts [8–23], were applied to compare the surface properties of samples before and after the catalytic testing. In a forthcoming paper the effect of Rh loading will also be addressed by the same techniques and, additionally, by EXAFS and XPS.

2. Experimental

2.1. Catalyst preparation

α-Al_2O_3 (12 m^2/g) was used as a thermally stable support. It was obtained by calcination in air at 1100 °C for 10 h of a commercial γ-Al_2O_3 (Puralox Sba-150, Sasol). Phase composition was verified by XRD. BET surface area amounted to about 12 m^2/g, with a pore volume of 0.4 cm^3/g.

Rh (0.5 wt.%) was deposited by three different techniques: grafting of the alumina surface with $Rh_4(CO)_{12}$, impregnation with $Rh(NO_3)_3$ and chemical vapor deposition (CVD) of $Rh(acac)(CO)_2$. In the following, the labels Rh/Al_2O_3(CB), Rh/Al_2O_3(NT) and Rh/Al_2O_3(CVD) will be used for catalysts prepared by $Rh_4(CO)_{12}$, $Rh(NO_3)_3$ and CVD of $Rh(acac)(CO)_2$, respectively.

The grafting procedure was described in detail elsewhere [2,24]. Briefly, the powders of α-Al_2O_3 were added to a solution of $Rh_4(CO)_{12}$ (Strem Chemicals) in excess *n*-hexane at room temperature, under magnetic stirring and inert N_2 atmosphere. The reaction was complete when the solution turned transparent (within 30 min). Catalyst powders were filtered under vacuum and dried at 60 °C for 2 h.

$Rh(NO_3)_3$ (a 14.68 wt.% solution in water, Chempur) was deposited onto α-Al_2O_3 via the incipient wetness technique. The impregnated support material was dried at 110 °C for 3 h.

$Rh(acac)(CO)_2$ precursor (Strem Chemicals) was purified by sublimation and stored under Ar before use. CVD was performed in a home-made rotary-bed CVD apparatus [25]. About 10 g of support were calcined 3 h at 500 °C under air, then were evacuated overnight at the same temperature. After cooling down to RT, 1/3 of Rh-precursor amount needed to obtain 0.5% loading was sublimed under Ar flow (10 mL/min of carrier and 10 mL/min of make-up) at 70 °C until complete sublimation has occurred. Then the sample was reduced at 500 °C under H_2 flow. This procedure was repeated twice in order to obtain the desired Rh loading.

For catalytic testing, the catalysts were deposited in the form of thin layers on ceramic tubular supports (O.D. = 4 mm); a dip-coating technique, illustrated in detail in a previous work [1,2], was applied at this scope. Briefly, a slurry is prepared by adding the catalyst powders to an acidic solution (HNO_3/powder = 1.7 mmol/g; H_2O/powder = 1.7 g/g) and is ball-milled for 24 h. Finally, ceramic tubes are coated on their terminal portions by dipping into the slurry and extraction at constant velocity. The coated tubes are then dried at 280 °C for a few minutes (flash-drying). Well adherent catalyst layers (5–6 mg, 10 to 20-μm thin, 22-mm long) were obtained.

Rh loadings were verified by atomic absorption and ICP-MS (Plasmaquad 3 VG ELEMENTAL) on solutions obtained after microwave dissolution of reduced catalysts in 2 mL of 1:1 HCl/HF mixture followed by residual HF elimination by gently boiling after adding HCl (3 mL × 1 mL). The measurements largely confirmed the nominal loads.

2.2. Testing apparatus

Reaction tests at high space velocity were carried out in a structured reactor with annular configuration. The reactor consists of an inner catalyst-coated ceramic tube, coaxially inserted into an outer quartz tube (I.D. 5 mm), giving rise to an annular duct through which the gas flows in laminar regime. The reactor was designed and the range of space velocities was chosen in such a way that the importance of mass transfer limitations was reduced and that the reactor operated far from equilibrium conditions, thus extending the useful temperature range for the kinetic investigation. Given the thermal equilibrium across the section of the ceramic tube, the temperature on the profile of the catalyst surface can be measured by sliding a thermocouple inside the internal ceramic tube [26]. Notably, effective dissipation of the heat of reaction by radiation allows realizing tests under quasi-isothermal conditions, as illustrated in [27].

A micro-GC (3000A by Agilent Technologies) was used to measure the inlet and outlet gas compositions. At each temperature, conversions and selectivities were estimated by repeated analyses, showing stable performances within 15–20 min.

Reference tests were performed at atmospheric pressure and at a gas hourly space velocity (GHSV) of 8×10^5 Nl/(kg_{cat} h). The feed mixture consisted of CH_4, O_2 and N_2 with composition: CH_4 = 4 vol.%, O_2/CH_4 = 0.56, N_2 to balance. During a typical run, the reactor temperature was increased from 300 °C up to 850 °C in step-wise increments of 10–50 °C. Blank experiments verified that homogeneous gas-phase reactions did not occur under these conditions.

Since only small amounts of powders could be recovered from the annular reactor after testing, insufficient for the characterization analyses, samples of the dried slurries, representative of the deposited layers, were also aged in a conventional packed-bed reactor, wherein the reaction was carried out at increasing temperature up to 850 °C (with a final hold of 4 h) with a standard feed mixture. The packed-bed reactor operated at much lower GHSV than the annular reactor (10,000 vs. 800,000 Nl/(kg_{cat} h)); however, this favoured the attainment of thermodynamically controlled conditions at 850 °C (complete conversion of reactants and over 95% selectivity of synthesis gas), that is the same conditions which established in the annular reactor after conditioning.

2.3. Characterization techniques

2.3.1. TPO/TPR experiments

They were performed to verify the inertness of α-Al_2O_3 to Rh inclusion, a phenomenon that is known to occur on γ-Al_2O_3 after high temperature oxidizing treatments [28]. Analyses were performed in a Thermo Electron Corporation TPD/R/O 1100 Catalytic Surface Analyzer. During TPO, the catalyst sample (dried slurry) was oxidized in flowing 2.06% O_2 in He, with a heating ramp of 7 °C/min from room temperature to a final temperature (this was varied between 300 and 900 °C) which was maintained for 1 h. Afterwards, the sample was cooled down to room temperature and subsequently reduced. The TPR measurements were carried out by heating from room temperature to 800 °C, at a rate of 10 °C/min in a flow of 4.78% H_2/Ar mixture (30 cm^3/min NTP).

2.3.2. H_2 chemisorption

A pulse technique [29] was applied to evaluate the dispersion of Rh that is the ratio between the number of surface metal atoms and the total number of metal atoms of the sample. Analyses were carried out in the Thermo Electron Corporation TPD/R/O 1100 Catalytic Surface Analyzer. The powders were pretreated according to the following procedure: (1) heating from room temperature to 150 °C (10 °C/min), 30 min hold, in flowing He (50 cm^3/min NTP); (2) reduction in pure H_2, 50 cm^3/min NTP, by heating up to 500 °C (10 °C/min), with 1 h hold; (3) purge in He, 50 cm^3/min NTP, 500 °C, hold 1 h; (4) cooling in He, 50 cm^3/min NTP, to room temperature; (5) pulse chemisorption (10–20 pulses) of 4.78% H_2 in Ar (sampling loop volume = 0.961 cm^3), in flowing Ar, 30 cm^3/min NTP, room temperature. The H_2-uptake was evaluated by comparing the intensity of the output pulses with the asymptotic intensity of pulses at saturation.

H_2/O_2 titration measurements were also performed for comparison. The technique involves the adsorption of oxygen on the reduced metal (with stoichiometry O/Rh = 1), followed by hydrogen titration of the chemisorbed oxygen [30,31]. The proposed stoichiometry is:

$$RhO + 3/2H_2 \rightarrow RhH + H_2O$$

Since the H/Rh ratio is 3/1, this technique provides a higher sensitivity than the traditional H_2 chemisorption technique. The procedure included the reducing pretreatments (1)–(4) as the traditional H_2-chemisorption technique; before injecting the series of H_2/Ar pulses these additional steps were introduced: (i) oxygen chemisorption in 2.06% O_2 in He, 50 cm^3/min NTP, at room temperature, 1 h hold (a sufficiently long time to guarantee saturation of the surface sites); (ii) purge in He, 50 cm^3/min NTP, room temperature, 1 h hold.

2.3.3. CO chemisorption

The use of CO as a probe-chemisorbing molecule was also investigated. After the reducing pretreatment (steps (1)–(4) as described above), several pulses of a CO/He mixture (5.03% volume fraction of CO) were injected at room temperature, in flowing He (20 cm^3/min NTP).

2.3.4. HRTEM

The morphology and distribution of the supported metal particles were evaluated by HRTEM micrographs. The powder samples (pre-reduced in H_2/N_2 = 20/80 flow at 500 °C and aged under CPO reaction conditions) have been further grinded and dispersed in isopropanol in an ultrasound bath. A drop of the suspension has been deposited on the carbon grid which, after solvent evaporation under vacuum, has been inserted in the column of the JEOL Jem-2010 EX high resolution transmission electron microscope. The instrument is equipped with an energy dispersive X-ray spectrometer—EDS (probe spot 5 nm). Pictures have been taken at 250,000–800,000× magnifications, spanning wide regions of several support grains in order to provide a well representative map of the catalyst system.

Distribution histograms of metal particles volumes versus diameters were evaluated from about 300 to 550 counts per sample.

2.3.5. CO-DRIFTS

The nature of the rhodium species, before (pre-reduced in H_2/N_2 = 20/80 flow at 500 °C) and after catalytic tests (aged samples), was investigated by diffuse reflectance infrared Fourier transform spectroscopy (hereinafter DRIFTS) using CO as probe molecule. Before admitting CO, catalysts were mildly reduced at 250 °C, in hydrogen flow, cooled down in He to RT, in order to ensure complete reduction of rhodium nanoparticles but avoiding any sintering of isolated Rh sites. The surface was then saturated with CO by injecting, in He flow, several 50 μL pulses of a mixture CO/Ar 50/50 by vol. Spectra were then recorded with a FTS-60A spectrophotometer using a home-made reaction chamber, the whole apparatus is described elsewhere [32]. The amount of chemisorbed CO was also quantified and could be compared with the independent results of CO pulse-chemisorption measurements.

3. Results

3.1. TPO/TPR

A systematic investigation was carried out over the Rh/Al_2O_3(CB) catalyst; the TPO temperature was varied between 300 and 900 °C. After each TPO, the TPR curve showed a H_2-consumption peak at about 100 °C. H_2-uptake was quantified and compared with the total number of Rh atoms; results are reported in Table 1. It is worth mentioning that a careful

Table 1
H_2-uptake/Rh load (mol/mol) in TPR after TPO at increasing temperatures

T TPO (°C)	H_2/Rh
300	1.76
400	1.51
500	1.40
600	1.39
700	1.12
800	1.36
900	1.38

calibration of the instrument with CuO samples was necessary at this scope. Still, uncertainty of the response factor was estimated at 10%. The measured H_2/Rh ratios were very close to the stoichiometric value 1.5 of Rh_2O_3 reduction. This suggests that oxidation of Rh was complete even after the oxidizing treatment at 300 °C.

The progressive decrease of H_2-uptake at increasing TPO temperature, that characterizes the Rh/γ-Al_2O_3 catalysts [28], was not observed. Inclusion of Rh within the α-Al_2O_3 support upon high temperature oxidation did not represent a significant phenomenon.

Analogous selected tests were also performed over the Rh/Al_2O_3 (NT) and Rh/Al_2O_3 (CVD) catalysts. Results confirmed that all the samples were easily oxidized and reduced, and the nature of Rh-precursor did not affect the stability of the support towards the sub-surface diffusion of Rh.

3.2. CH_4 partial oxidation tests in annular reactor

3.2.1. Conditioning and steady-state activity of Rh/Al_2O_3(CB) and Rh/Al_2O_3(NT)

In previous papers [1,2], we have reported that, over the 0.5% Rh/Al_2O_3(CB) and Rh/Al_2O_3(NT) catalysts, steady-state partial oxidation performances were obtained after an initial conditioning process. Those results are partly reported in Fig. 1; the phenomenon was especially evident for Rh/Al_2O_3(NT) samples, but a similar (though less pronounced) trend was shown by the Rh/Al_2O_3(CB) samples. During repeated standard runs at 800,000 Nl/(kg_{cat} h), a progressive increase of the high temperature catalyst activity (above 500 °C) was typically observed. The progressive activation eventually led to extremely high conversion/selectivity values, which closely approached the thermodynamic equilibrium thresholds at the highest investigated temperatures. The final stable activity is reported in Figs. 2 and 3, which replicate and extend previous kinetic investigations over the two catalysts [1,2,27]. In both cases, the reaction of methane and O_2 initiated at about 350 °C. At the reference space velocity of 800,000 Nl/(kg_{cat} h), O_2 conversion rapidly grew with temperature and was complete at about 500 °C. At lower temperatures, only deep oxidation products (CO_2 and H_2O) were observed in the product mixture, at higher temperatures CO and H_2 were formed at their selectivity increased significantly with temperature. At increasing space velocity, the decrease of reactants conversion was accompanied by a decrease of the syngas selectivity, which confirmed that H_2 and CO were secondary products.

3.2.2. Conditioning and steady-state activity of Rh/Al_2O_3(CVD)

Fig. 4 reports the results of three consecutive CPO runs over the fresh Rh/Al_2O_3(CVD) catalyst. Differently from the other samples, the catalyst did not undergo any appreciable evolution. Its initial activity was very high at all temperatures; conversions and selectivities kept almost unchanged after repeated experiments, except for a minor decrease of the low temperature conversion of CH_4.

At increasing space velocity, as shown in Fig. 5, the conversion of reactants significantly decreased. At 2×10^6 and 4×10^6 Nl/(kg_{cat} h), the conversion of O_2 did not reach 100% but established at asymptotic trends, typical of a mass transfer limited regime. The selectivity of CO was moderately affected by the increase of space velocity, while the selectivity of H_2 decreased more significantly with increasing GHSV.

At the intermediate GHSV value of 2×10^6 Nl/(kg_{cat} h) (at which the control of thermodynamics on the process was weakened), CPO runs were carried at increasing O_2/C ratios. Results are reported in Fig. 6. Upon increasing the O_2-feed content, the conversion of O_2 decreased, the conversion of methane kept unchanged at temperatures lower than 550 °C, while it moderately increased at higher temperatures. The

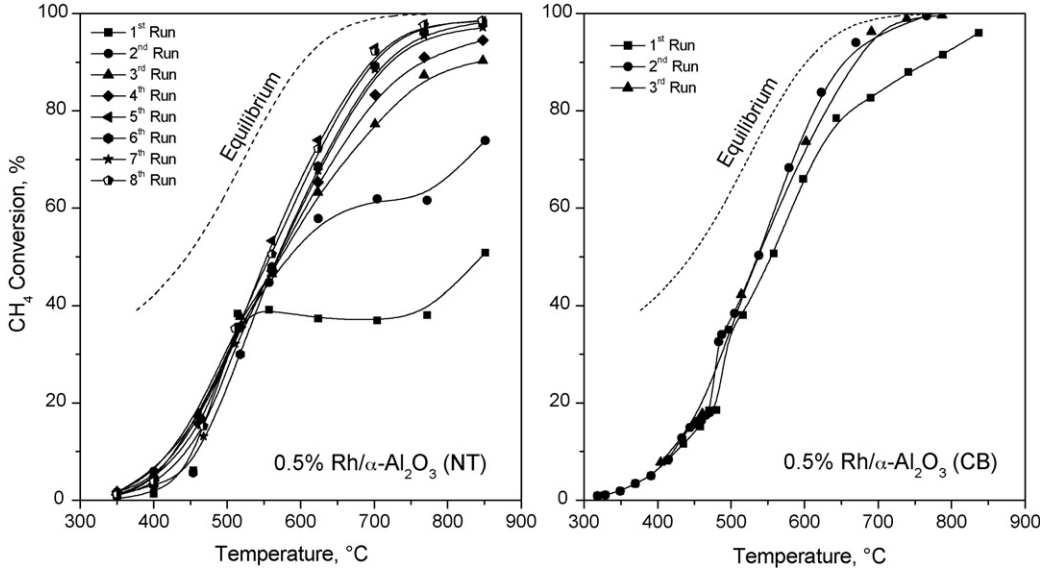

Fig. 1. Conditioning of Rh/Al_2O_3(NT) and Rh/Al_2O_3(CB) during successive CH_4-CPO runs, see also [1]. Operating conditions: CH_4 = 4%, O_2/CH_4 = 0.56, N_2 to balance, GHSV = 800,000 Nl/(kg_{cat} h). Dotted line = calculated thermodynamic equilibrium.

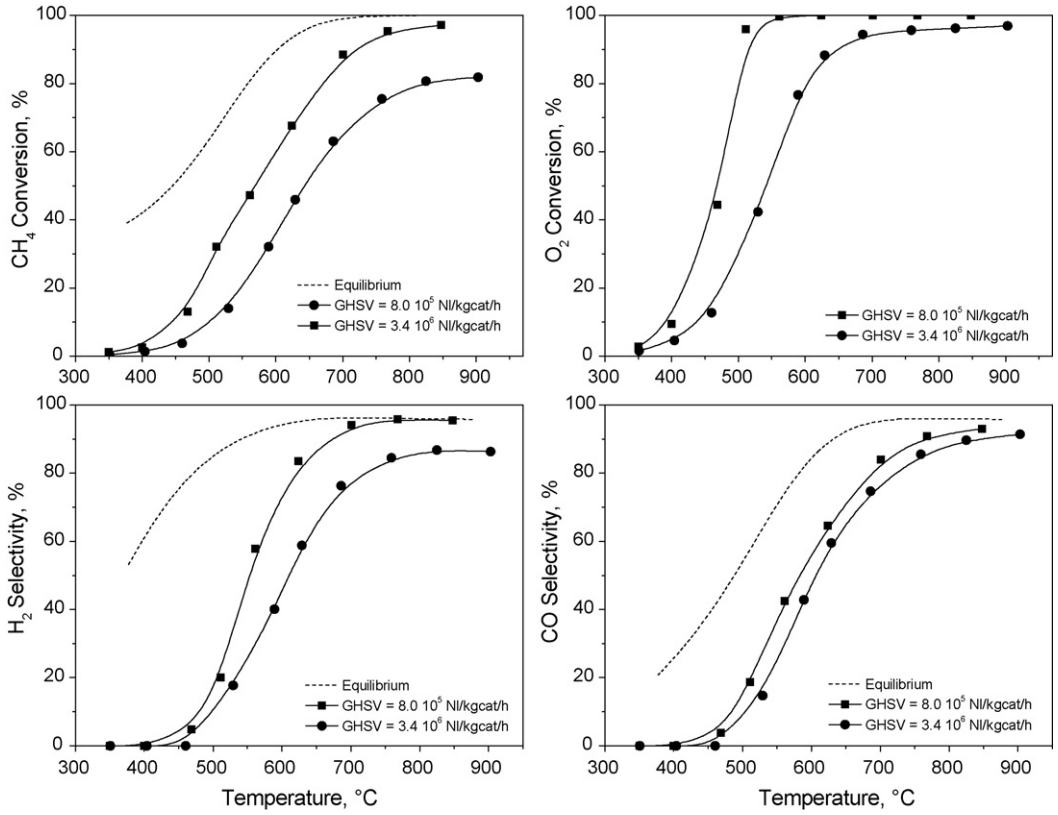

Fig. 2. 0.5% Rh/Al_2O_3(NT) catalyst after conditioning. Effect of space velocity. Feed composition as in Fig. 1.

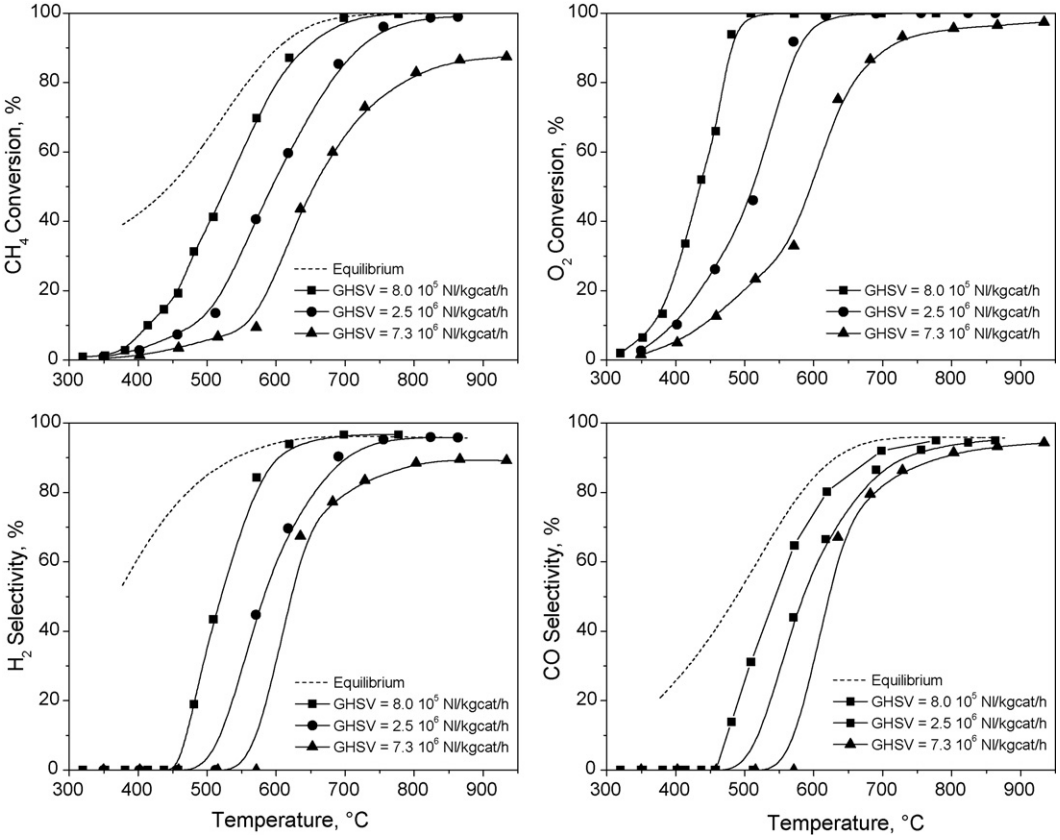

Fig. 3. 0.5% Rh/Al_2O_3(CB) catalyst after conditioning. Effect of space velocity. Feed composition as in Fig. 1.

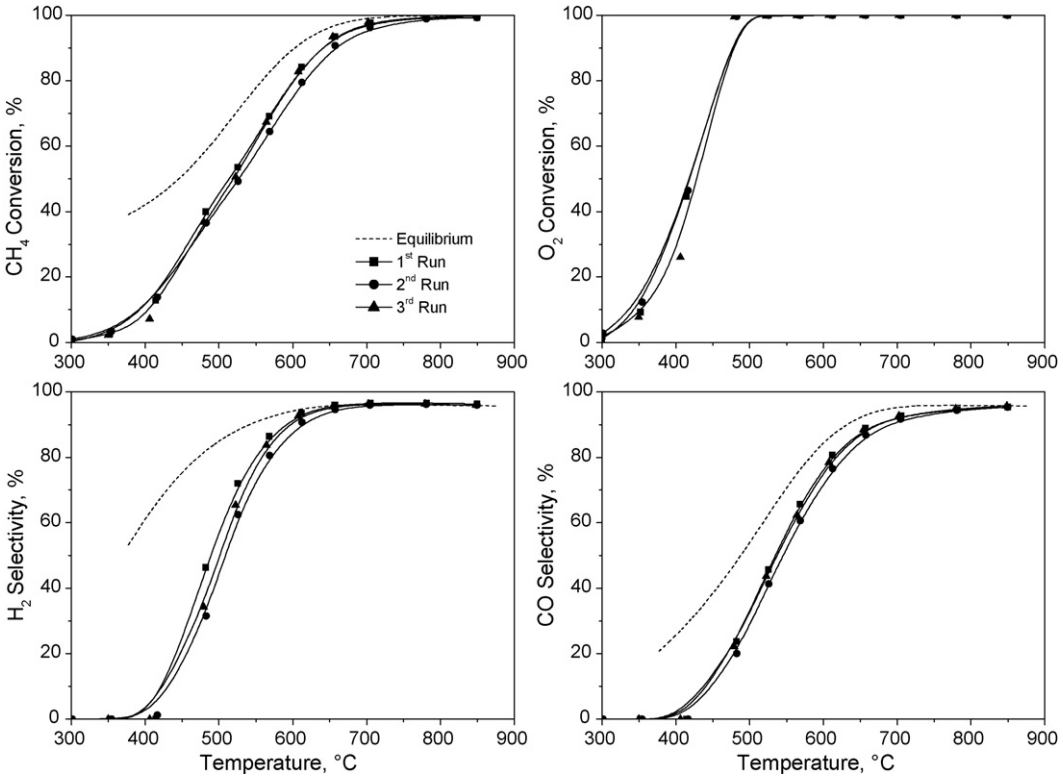

Fig. 4. Conditioning of Rh/Al_2O_3(CVD). Operating conditions: CH_4 = 4%, O_2/CH_4 = 0.56, N_2 to balance, GHSV = 800,000 Nl/(kg_{cat} h). Dotted line = calculated thermodynamic equilibrium.

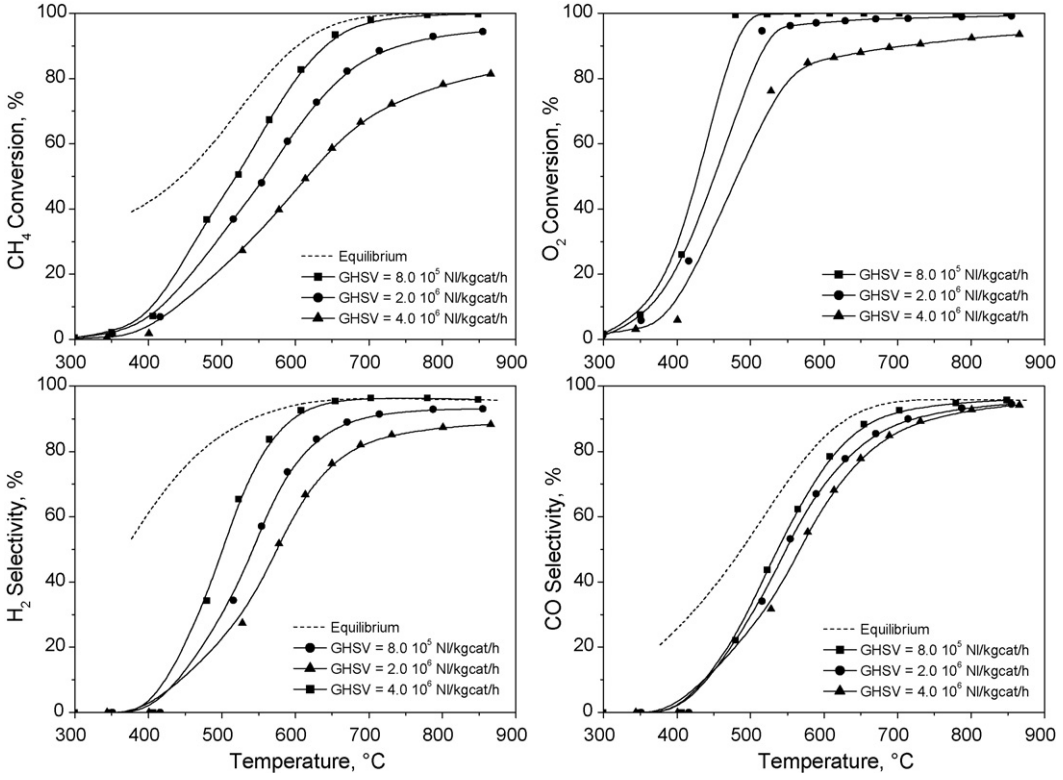

Fig. 5. 0.5% Rh/Al_2O_3(CVD) catalyst after conditioning. Effect of space velocity. Feed composition as in Fig. 1.

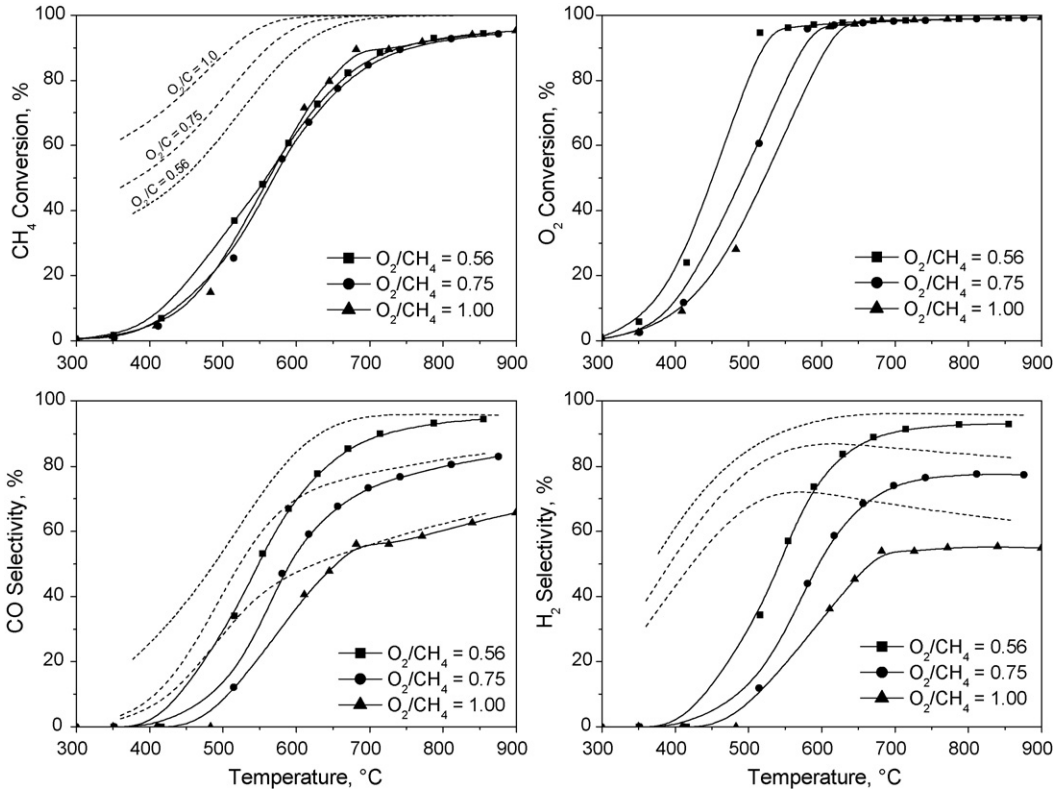

Fig. 6. 0.5% Rh/Al_2O_3(CVD) catalyst after conditioning. Effect of O_2/CH_4 feed ratio. CH_4 = 4%, N_2 to balance, GHSV = 2,000,000 Nl/(kg_{cat} h).

formation of CO and H_2 was shifted to higher temperatures and, as expected, it decreased at increasing O_2/C ratio.

In all the experiments, the measured axial temperature profiles had typical features. They were characterized by the presence of a hot-spot at the very beginning of the catalyst layer which decreased in intensity and migrated from the ending catalyst section (at the lowest reaction temperatures) towards the inlet section of the bed at increasing temperature (and syngas selectivity); in line with previous observations [27] this was interpreted as an evidence of the existence of an exo–endothermic reaction sequence.

3.3. Chemisorption of probe molecules

The results of the chemisorption measurements are reported in Table 2. In the case of the Rh/Al_2O_3(NT) catalyst, a H/M ratio of 0.38 was estimated by H_2 chemisorption over the fresh pre-reduced catalyst. Notably, the measured CO/Rh ratio amounted to 0.72 according to the CO pulse-chemisorption analysis. Both results were confirmed by independent techniques (the H_2/O_2 titration and the CO-DRIFTS analysis, respectively). The effect of the ageing treatment under reaction condition was apparently negligible according to H_2 chemisorption (H/Rh = 0.36). However, after ageing, the measured CO/M ratio decreased significantly, amounting to 0.4 according to the pulse-chemisorption technique (still supported by the CO-DRIFTS analyses).

In the case of the Rh/Al_2O_3(CB) catalyst, the estimated H/M ratios prior and after ageing under reaction conditions were similar to those estimated for the Rh/Al_2O_3(NT) sample. The CO/M ratio was higher than the H/M ratio for the fresh catalyst, but was comparable to it for the aged sample.

In the case of the Rh/Al_2O_3(CVD) catalyst, a H/M value of about 0.5 was estimated by H_2 chemisorption. The same technique indicated that no appreciable change of the metal surface occurred after ageing under reacting conditions. Also, contrarily to other samples, a close match between CO/M and H/M ratios was found.

Table 2
Results of H_2 chemisorption and CO chemisorption

	H/M		CO/M	
	Reduced@500 °C	CPO@850 °C	Reduced@500 °C	CPO@850 °C
CVD	0.52	0.47	0.51	0.38
CB	0.33	0.35	0.70	0.31
NT	0.38	0.36	0.72	0.40

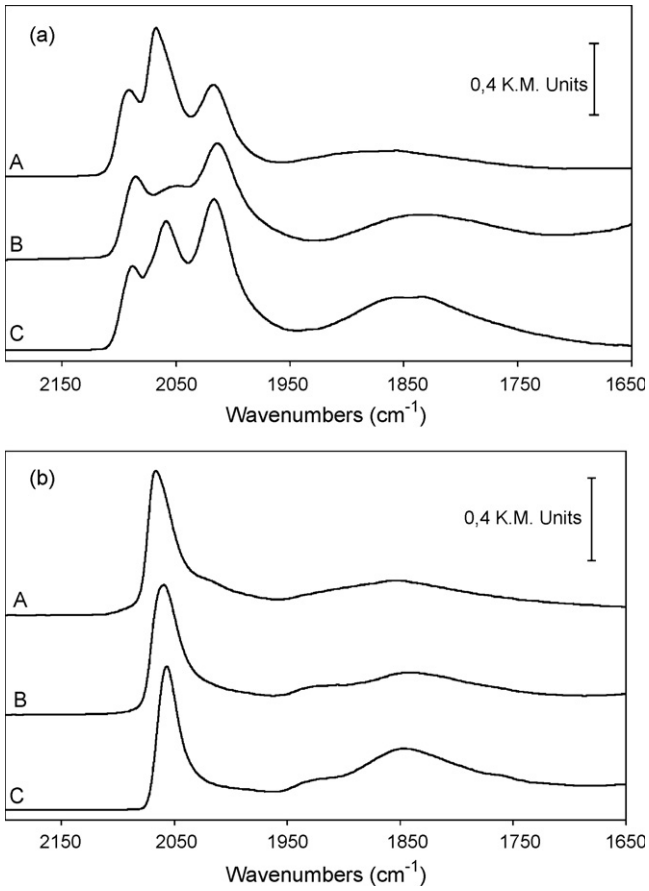

Fig. 7. CO pulses-DRIFT spectra. (A) Rh/Al_2O_3(CVD); (B) Rh/Al_2O_3(CB); (C) Rh/Al_2O_3(NT). (a) Reduced samples and (b) aged samples.

3.4. CO-DRIFTS

The CO-DRIFTS experiments (Fig. 7) showed some general features: the presence, in the pre-reduced samples, mainly of CO absorption bands typical of $Rh(I)(CO)_2$ gem-dicarbonyl species (doublet located approximately at 2090 and 2015 cm^{-1}) and of Rh(0) nanoparticles (linear CO absorbing around 2060 $cm^{-1}$and bridging CO around 1870 cm^{-1}) [12–16,21,32–37]. In aged samples an increase of bands related to CO chemisorbed on metallic particles was observed with respect to isolated $Rh(I)(CO)_2$ sites.

The DRIFT spectrum of the pre-reduced Rh/Al_2O_3(NT) sample shows the presence of bands located 2047 and 1831 cm^{-1} ascribable, respectively to CO adsorbed linearly and bridged on Rh(0) particles, and of bands located at 2084 and 2012 cm^{-1} typical of gem-dicarbonyl species.

In the pre-reduced Rh/Al_2O_3(CVD) sample, the gem$(CO)_2$ doublet is located at 2091 and 2017 cm^{-1}, whereas linear and bridged CO on metal particles absorptions fall, respectively, at 2067 and 1865 cm^{-1}. Rh/Al_2O_3(CB) sample, after CO pulses, shows the presence of the $Rh(I)(CO)_2$ doublet bands located at 2085 and 2010 cm^{-1} and of linear CO band at 2052 cm^{-1} and bridged at 1830 cm^{-1}.

Aged samples, if compared with fresh ones, show a more homogeneous pattern of adsorbed CO absorption bands. The main difference between fresh and aged samples is represented by the increase of bands due to CO adsorbed on Rh(0) metallic particles in the latter respect to geminal CO on isolated Rh(I) sites. In other words a significant sintering of isolated Rh(I) sites has occurred leading to small metal particles (as also evidenced by HRTEM measurements); all the samples show almost only the presence of IR bands of CO adsorbed on metal nanoparticles.

In aged samples, apart previously described bands, is also present a band located around 1935 cm^{-1}, that can be ascribed to $Rh_2(CO)_3$ species [33,38,39].

Curve fitting was carried out. Table 3 reports the ratio between the amount of linearly chemisorbed CO on Rh^0 and the amount of gem-$(CO)_2$ ratio, which is commonly treated in the literature as a measure of the relative abundance of Rh nanoparticles with respect to Rh^+ isolated and/or on Rh clusters sites [39]. Estimates of the ratio between linearly and bridged CO ratio are also reported in Table 3; linear to bridged CO ratio is usually considered as a indicator of particles dispersion [40] and/or morphologies.

3.5. HRTEM

The results are reported in Fig. 8, in the form of histograms.

The particle volume distribution of the fresh Rh/α-Al_2O_3(NT) sample shows a single component centered at 1.2 nm. Particles with measured diameters up to 0.7–0.9 nm correspond actually to clusters of 10–20 atoms, only for higher diameters the total atom number can account for three-dimensional particles (in fcc packing the smallest regular polyhedron, corresponding to a two atoms edge, has a diameter of 0.8 nm and consists of 13 atoms). The morphology of most particles is well described by the truncated cubo-octahedron model with the 111 plane in contact with the support. The HRTEM images show that the vast majority of metal particles

Table 3
Curve fitting of the CO-DRIFTS spectra

	CO_{lin}/CO_{br}		$CO_{Rh(0)}/CO_{Rh(I)}$	
	Reduced@500 °C	CPO@850 °C	Reduced@500 °C	CPO@850 °C
CVD	1.51	0.33	0.88	–
CB	0.40	0.30	0.12	–
NT	0.36	0.27	0.31	–

CO_{lin}/CO_{br} and $CO_{Rh(0)}/CO_{Rh(I)}$ are, respectively the ratios between integrated intensities (as obtained from fitting procedure) of linear and bridged CO adsorbed on Rh(0) nanoparticles and between linear CO adsorbed on Rh(0) nanoparticles and geminal dicarbonyl on Rh(I) sites.

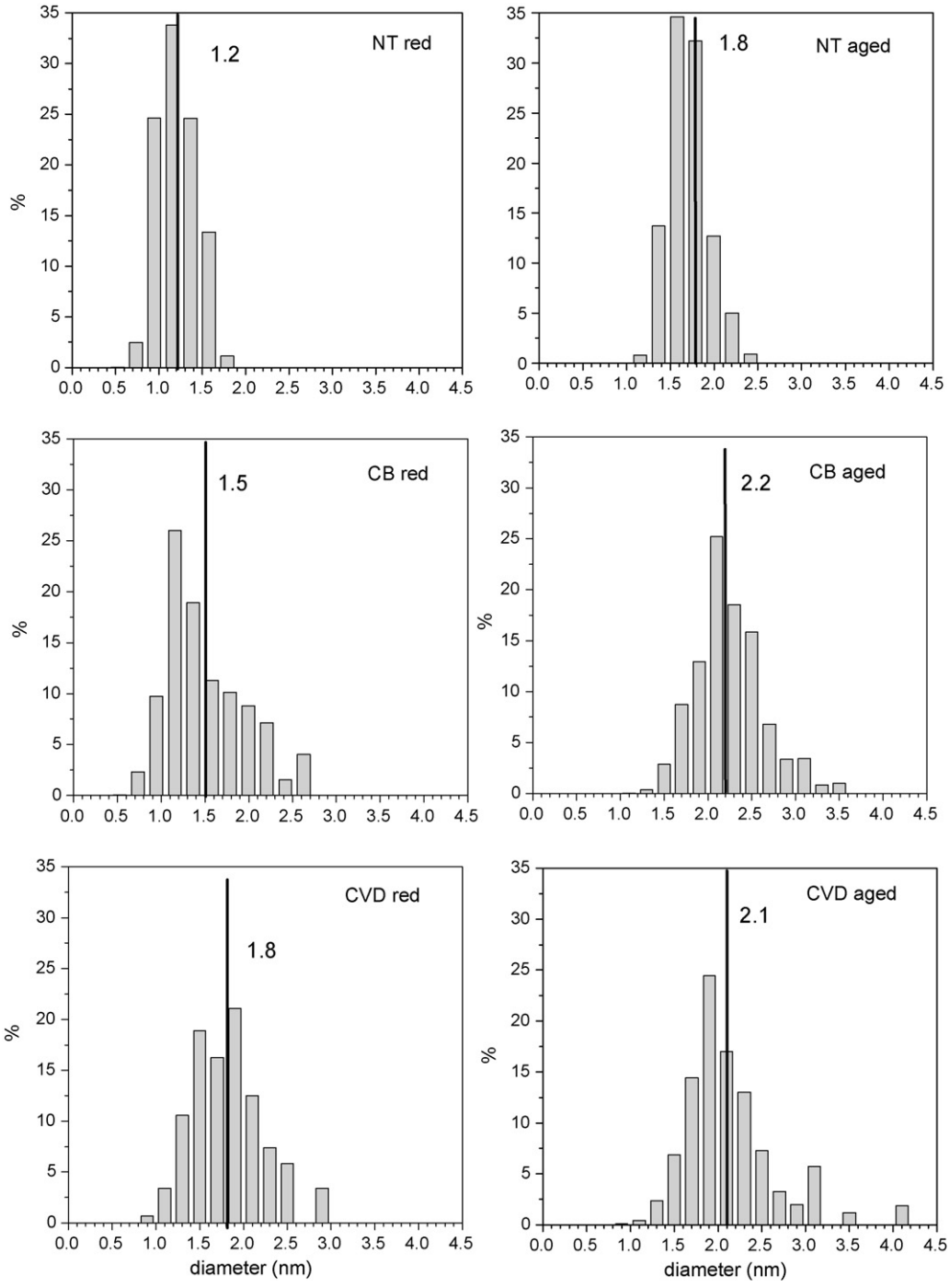

Fig. 8. HRTEM volume distribution histograms of reduced and aged 0.5% Rh/Al_2O_3 (NT), 0.5% Rh/Al_2O_3 (CB) and 0.5% Rh/Al_2O_3 (CVD). Estimates of the mean particle size are reported.

has a well defined hexagonal geometry habit and, where the size is sufficient to clearly resolve the diffraction fringes (3 nm diameter), 111 crystal planes are well recognizable, in agreement with the Rh fcc packaging in octahedral growth geometry. Relevant images are reported in Fig. 9.

In the sample Rh/α-Al_2O_3(NT) after ageing the particle size distribution is narrow and symmetrical with a mean diameter of 1.8 nm. The fraction of particles with diameters of 0.7–0.9 nm has disappeared and bigger crystallites are visible up to about 2.5 nm, so that the average particle size present in the reduced sample is increased under ageing. No carbon deposit is visible on the catalyst surface, neither it is detectable with the EDS probe.

The particle distribution function of the fresh Rh/α-Al_2O_3(CVD) sample shows a main broad component, centered at 1.8 nm and a few larger particles (with diameters in the 3–5 nm range) accounting for about 13% of the total metal atoms. The average diameter of the reduced metal particles prepared

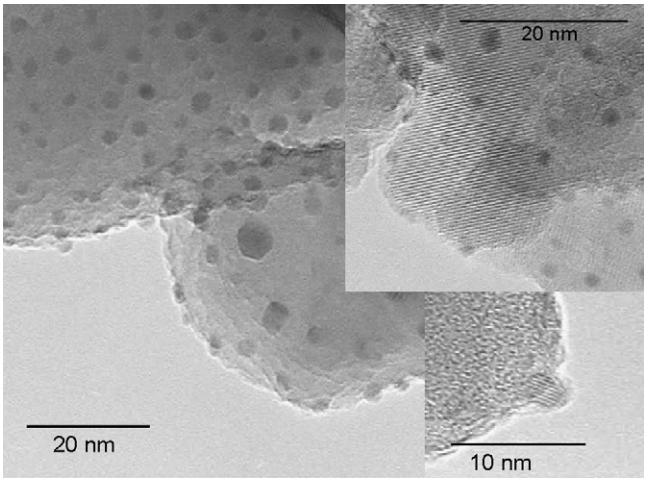

Fig. 9. HRTEM micrographs of the reduced 0.5% Rh/Al_2O_3(NT) sample taken at different magnifications.

by CVD corresponds to the average size obtained after ageing of the nitrates preparation route. The morphology of metal particles is mostly spherical.

After ageing of the Rh/α-Al_2O_3(CVD) catalyst, the particle size distribution is narrow and symmetrical and the average diameter size is only slightly increased with respect to the reduced system to a value of 2.0 nm with no more than a 18% fraction of the total metal atoms in particles greater than 3.0 nm. That is, ageing does not significantly affect the metal particles size in the case of the CVD preparation route.

The sample Rh/α-Al_2O_3(CB) shows a particle size distribution as narrow as in the nitrates reduced sample and with an average diameter is of 1.5 nm, intermediate between the nitrates and CVD systems, as well as the metal particle and the support morphology.

In the same sample Rh/α-Al_2O_3(CB) after ageing the particle size distribution is still narrow and symmetrical with but the mean diameter has increased to 2.2 nm. The fraction of bigger crystallites is visible up to about 3.0 nm, so that the overall particle size is appreciably larger after ageing than in the reduced sample.

4. Discussion

4.1. Morphology of the supported Rh particles (HRTEM vs. CO-DRIFTS)

The morphology of the larger Rh particles (>1–1.5 nm) is clearly recognized from HRTEM images: truncated cubo-octahedron in the cases of catalysts prepared via impregnation or grafting of α-alumina (NT and CB), spherical (cubo-octahedron) in the case of the largest particles obtained by CVD methodology.

The same truncated cubo-octahedron model was proposed by Bernal et al. [18,19] to explain the growth of Rh nanoparticles over ceria, on the basis of experimental and simulated HRTEM images. In those works, the examined smallest particle size corresponded to 1 nm and the mean particles sizes ranged between 2.2 and 6.6 nm, depending on the reduction temperature, being 3.3 at 773 K pre-reduction temperature. Kaspar and co-workers [20] also assumed a truncated cubo-octahedron geometry for evaluating the dispersion of 2.4–4.2 nm Rh particles (supported on ceria-zirconia) from HRTEM images.

The peculiar morphology exhibiting a large planar face is in perfect agreement with the coexistence of the linear and bridged CO adsorption modes, observed by DRIFTS. Since bridged CO occurs mainly on flat facets, the linear to bridged adsorption ratio is expected to be lower on samples with a high amount of truncated octahedron particles exposing mainly 111 facets. The Rh/Al_2O_3(NT) sample shows a relatively low linear to bridged CO ratio; on the other hand the Rh/Al_2O_3(CVD) sample, where bigger and well formed three-dimensional nanoparticles are present according to HRTEM, shows the highest linear to bridged ratio. However such remarkably high value ($CO_b/CO_l = 1.5$) can be overestimated due to the broadness of bridged CO band. The features of the Rh/Al_2O_3(CB) sample are similar to those of the Rh/Al_2O_3(NT) sample according to both techniques.

Concerning the smaller particles (with size lower than 1 nm), which are present in significant amount over the NT and CB catalysts, the HRTEM images do not allow to recognize their geometry, but show a very weak contrast. Besides, HRTEM cannot detect isolated Rh atoms, whose presence on the pre-reduced samples is suggested by the CO-DRIFTS experiments. It is believed that the model of the truncated cubo-octahedron still applies, but it tends to reduce, in the smallest aggregates, to that of raft, that is a two-dimensional aggregate of Rh atoms with expectedly weak metallic character; the presence of rafts in turn is congruent with the existence of Rh atoms and/or very small metal particles (clusters) strongly interacting with the support, as detected by IR-spectroscopy. Such isolated atoms and/or very small metal particles can be easily converted in $Rh^I(CO)_2$ sites upon CO adsorption as already reported for Rh/α-Al_2O_3(CB) and Rh/α-Al_2O_3(NT) samples [8] according the reaction:

$$(1/x)Rh_x^0 + 2CO + OH^- \rightarrow Rh^I(CO)_2 + 1/2H_2 + O^{2-} \quad (1)$$

leading to $Rh^+(CO)_2$ species bonded to alumina surface (AlO–$Rh(CO)_2$ and/or $(AlO)_2$–$Rh(CO)_2$) [41]. Indeed a small amount of surface hydroxyls was detected over the present α-Al_2O_3 support [8], thus reaction (1) may have contributed to the formation of isolated species.

The assumption of two-dimensional growth for the smallest Rh particles is partly in contrast with the simulations of Bernal et al. [19], who proposed the adequacy of the truncated octahedron model down to 1 nm aggregates, without distinction between metal particles and aggregates of few atoms. However, the two-dimensional growth of Rh particles over ultradispersed systems was already reported in the literature. Investigating the morphology of ultradispersed Rh particles on γ-alumina by chemisorption, IR-spectroscopy and TEM, Yates et al. [9,10] concluded that Rh nanoparticles are organized as two-dimensional rafts (one atom thick), and estimated that 1.5 nm rafts contain in average eight Rh atoms. By H_2

chemisorption, TPO/TPR experiments and TEM, Prins and co-workers [11] showed the presence of two kinds of Rh/Rh_2O_3 particles on TiO_2: the first kind consisted of raft particles, easily reduced/oxidized and with high dispersion, the second kind consisted of spherical particles, harder to reduce/oxidize and with low dispersion. Several authors, then, have reported very high dispersions for Rh particles over catalysts at extremely low metal content and such high dispersions are of course in contrast with an important three-dimensional growth [16,17].

The different precursors and preparation techniques give rise to a different balance of metal particles and isolated Rh(I) sites: CO-DRIFTS spectra show that the CVD samples has the highest metal particles to isolated sites ratio. This can be attributed to the peculiar multi-step preparation technique, in which the repeated reducing treatments in between the CVD phases seem to be effective in a ''gentle'' sintering of Rh sites giving rise to well formed metal nanoparticles; the metal sites, in turn, catalyze the $Rh(acac)(CO)_2$ decomposition to metallic atoms and promote the particle growth. These combined effects likely prevent the formation of randomly sized particles and isolated sites, while it favours the formation of evenly and well formed nanoparticles.

On the opposite, the samples prepared starting from the organometallic $Rh_4(CO)_{12}$ precursor and the inorganic $Rh(NO_3)_3$ precursor show less homogeneous surfaces, where high concentrations of isolated sites and small raft-like metal particles coexist with three-dimensional particles. Maramoto-Valienete et al. [22] have characterized by microcalorimetry the surface of Rh/Al_2O_3 catalysts obtained by incipient impregnation of the support with a solution of $RhCl_3$; the Rh catalysts evidenced a high heterogeneity of the surface sites for the adsorption of hydrogen and the coexistence of three modes of CO adsorption (linear, gem-dicarbonyl and bridged).

After ageing, the differences among samples tend to vanish; all samples show a linear to bridged ratio of about 0.33, an important loss of isolated species and very small particles, a growth of the average particle size up to about 2 nm (a significant growth in the case of the carbonylic and the inorganic Rh precursors, a modest growth in the case of the CVD sample). Apparently, the high temperature reaction drives the surface changes towards the reaching of a common stable state, wherein the Rh metal particles are more uniformly sized and shaped. This conclusion is in line with the findings of Finocchio et al. [8] who addressed a FT-IR study on the effect of selected pretreatments over the same $Rh/\alpha\text{-}Al_2O_3$ (NT) catalyst; they observed that heating the sample in a CH_4/O_2 mixture (mimicking the CPO reaction conditions) favoured the formation of more structured Rh particles and reduced the initial heterogeneity of the surface (observed after outgassing in He). Besides, the result is in line with the evidence that adsorption of gas-phase species can cause reconstruction of Rh and other metallic substrates [42]. In field ion microscopy studies, Kruse et al. [43,44] have shown that adsorption of CO or O_2 can induce morphological changes of Rh particles with formation of densely packed planes, and that defect sites like kinks (characteristic of small clusters) are especially mobile. It was shown that this process is thermally activated [43]. Disruption of Rh–Rh bonding upon CO adsorption onto highly dispersed Rh particles was detected using EXAF spectroscopy by Bando et al. [45]. Concerning the effect of high reaction temperatures, Bulushev and Froment [14] have described the process of Rh growth by thermal sintering as the progressive agglomeration of small clusters into metallic particles and the reshaping of metallic particles into three-dimensional structures with smooth surfaces.

Initial and final states of the surface were very close in the case of the CVD sample, while the reconstruction was more important for the CB and the NT samples.

The features of catalyst reconstruction herein proposed seem partly in contrast with the findings of Grunwaldt et al. [46] who investigated by *in situ* EXAFS the effect of several treatments, including CPO reaction conditions, on the coordination and morphology of Rh particles. They found that structural transformation occurred at the ignition of the CPO reaction, with abrupt reduction and re-dispersion of the Rh particles. However, the authors studied catalysts at relatively high Rh content (5%) characterized, after reduction in H_2, by the formation of 6 nm particles. It cannot be excluded that the initial presence of ''large'' particles produces opposite reconstruction patterns than those herein observed for very small aggregates.

4.2. Metal dispersion (chemisorption vs. HRTEM and DRIFT)

The responses of the different chemisorption techniques show some scattering; the H/M ratios are in some cases (the reduced CB and NT samples) lower than the CO/M ratios. Such disagreement can be explained by assuming, in line with Wong and McCabe [28], that isolated Rh atoms, which chemisorb two CO molecules each, cannot dissociatively chemisorb the H_2 molecule. Such an assumption deserves a more general comment; it seems, in fact, in contrast with the results of Prins and co-workers [12], who widely treated the issue of H_2 adsorption stoichiometry over small Rh particles supported over high surface area aluminas. They found that, when accounting for both strongly adsorbed and weakly adsorbed H_2, H/M ratios higher than unity are observed; the multiple adsorption on the exposed metal atoms was associated to formation of weak polyhydride complexes over partly charged Rh atoms (as those contained in small clusters are). More recent experimental and theoretical studies [48] have confirmed that chemisorbed H_2 can exceed the monolayer amount, with an overall H:Rh stoichiometry >1; it has been shown, however, that this is an integral result which derives from the contribution of strongly bonded H–Rh species (with thermal desorption temperature of 300–400 K) and the contribution of weakly bonded H_2–Rh species (with desorption temperature of 100–200 K). It must be recalled now that the pulse technique herein applied intrinsically accounts for the unique formation of ''irreversibly chemisorbed species'' [29] or, more appropriately [12], of strongly bonded H–Rh species.

CO-DRIFT spectra of the fresh samples show that isolated Rh(I) species are present in large amount over the CB and NT

samples, in minor amount over the CVD sample. Indeed, considering the fresh CVD sample, a good match between H_2 chemisorption and CO chemisorption measurements was found (CO/M = H/M = 0.5); in this case metallic particles prevail over isolated species and the main CO chemisorption stoichiometry is CO:Rh = 1:1, since linearly bonded CO largely prevail on bridged bonded CO. Ageing had a little effect on the chemisorption results, which is also in line with the indications from HRTEM and CO-DRIFT of a moderate sintering of the metal particles.

In the cases of the fresh Rh/Al_2O_3(CB) and the fresh Rh/Al_2O_3(NT) samples, the chemisorption measurements confirm (in line with the other characterization techniques) that the two systems are similar; a CO/M ratio of about 0.7 and a H/M ratio of about 0.35 were measured in both cases. The fact that the amount of chemisorbed CO was twice as much the amount of chemisorbed H can be explained by the large fractions of isolated Rh(I) species initially present on the surface. After ageing, the CO/M ratios halved, while the H/M kept almost constant; thus a close match from the two techniques was found. HRTEM and CO-DRIFTS indicate that under reaction conditions a mild sintering of particles and loss of isolated species and very small aggregates occurred. These two effects apparently counterbalanced in the case of H_2 chemisorption (more Rh atoms became available to dissociative chemisorption, but the overall metal surface decreased), while both concurred to decrease the CO-chemisorption capacity.

Finally, the congruence between the results of the chemisorption measurements and the particle size distributions measured by HRTEM was verified. In the case of the NT sample (wherein the model of spherical particles is highly inappropriate) dispersion was independently estimated assuming a geometric model of raft truncated octahedrals, that is hexagonal prisms with the basal plane corresponding to the hexagonal planar projection of the truncated octahedron 111-face of the fcc crystal and a height/diameter ratio of 1/3. Note that the lower the height/diameter ratio, the lower the exposed surface per volume. The ratio value of 1/3 has been chosen as the lowest possible able to accommodate at least three atomic layers also for the smallest measured diameters. Dispersions were calculated as the ratio between the number of Rh atoms accommodated in the first monolayer (in fcc packing) at the external surface (not in contact with the support) of the prism and the total number of atoms in the prism volume for any measured diameter. The obtained values have then been averaged over the volume distribution histograms. Dispersions of 0.65 and 0.54 were evaluated for the fresh and aged surfaces. The qualitative match with the H/M and CO/M measurements is satisfactory when considering that H_2 chemisorption is expected to underestimate the dispersion in the presence of isolated species, CO chemisorption is expected to overestimate the dispersion in the case of adsorbed di-carbonyls (isolated species).

Similar results (0.58 and 0.45 calculated dispersions) were obtained for the fresh and aged samples, prepared by grafting. In the case of the CVD sample, the dispersions evaluated by HRTEM amount to 0.47 for the fresh and aged samples, in close agreement with the chemisorption results.

Assuming the geometrical model of rafts and based on the HRTEM results, it was estimated that only few percentages of the alumina surface was occupied by the Rh particles, thus the surface density of Rh was relatively low despite the use of a low surface area support.

It is noted that the good match among independent techniques is extremely valuable; it is in fact known in the literature [12,21] that hydrogen chemisorption measurements may not be conclusive for the determination of the metal surface area in highly dispersed system. Prins and co-workers [12] have calibrated the chemisorption measurements with EXAFS measurements, which provided estimates of the metal average coordination number. H_2 chemisorption combined with HRTEM and EXAFS measurements were applied by Vlaic et al. [21] to study the morphology of rhodium particles in a 5% $Rh/Ce_{0.5}Zr_{0.5}O_2$ catalyst. We also applied EXAFS (a proven technique for studying the oxidation state, identity of neighbouring atoms and particle size of Rh [12,45–47]) in concert with the herein illustrated techniques for characterizing catalysts at high Rh loading and the results will be presented in a dedicated paper.

4.3. Catalytic behaviour

After an initial conditioning process, whose features are better discussed in the following, the different catalyst formulations reached stable performances, characterized by very high conversions and selectivities, which were little affected by the preparation methodology. Both qualitatively and quantitatively, in fact, the different catalysts showed a common behaviour. Under reference operating conditions, the equilibrium was reached at about 700 °C. At increasing space velocity, the approach to thermodynamic equilibrium weakened and the decrease of methane conversion was accompanied by a decrease of syngas selectivity. All samples, thus, provided evidence for an indirect kinetic scheme, wherein CO_2 and H_2O are primary products of methane deep oxidation and CO and H_2 are secondary products of methane reforming. This indirect pattern to synthesis gas has been recently supported by spatially resolved analysis of the reacting mixture in autothermal experiments with Rh-coated foams [49]. In line with recent works by Wei and Iglesia [4,5], previous kinetic investigations on methane CPO over Rh/Al_2O_3(CB) and Rh/Al_2O_3(NT) catalysts [1,2,27] indicated that over both systems the rate of CH_4 oxidation and the rate of CH_4 reforming are proportional to methane partial pressure but do not depend on the amount of the co-reactant (O_2 and H_2O). In this work, the investigation was extended to the Rh/Al_2O_3(CVD) catalyst; focused experiments on the effect of the O_2/CH_4 ratio showed that also in this case the low temperature conversion of methane (related to the kinetics of deep oxidation) was unaffected by an increase of O_2 concentration, and the high temperature conversion of methane (related to the kinetics of steam reforming) was independent on the amount of H_2O (which increased at increasing O_2/CH_4 feed ratio).

The fact that the different catalysts showed similar performances is not surprising, as it agrees well with the

results of the various characterization techniques according to which the morphology and dispersion of the catalysts after high temperature reaction are similar.

Instead, important differences were shown by the initial catalytic behaviour of the three systems which underwent different evolutions. The Rh/Al_2O_3(NT) catalyst showed the lowest initial activity (at high temperature) and a slow progressive activation, the Rh/Al_2O_3(CB) catalyst had a relatively high initial activity and its conditioning process completed in a shorter time, Rh/Al_2O_3(CVD) catalyst showed a very high initial activity, which practically kept constant during repeated runs. The duration of the conditioning process seems thus strictly related to the extent of the surface reconstruction from a fresh surface, whose degree of heterogeneity depends on the preparation procedure, to a final state wherein a more evenly organized surface establishes. It is worth noting that the absence of a conditioning process, that is the observation of very high and stable performances from the initial CPO run, was recently reported for embedded Rh particles in alumina matrix, that is for a Rh-catalyst with highly homogeneous surface species [17].

In a previous study on the conditioning of Rh/Al_2O_3(NT) catalysts, the evolution of CPO activity, and the results of CH_4 pyrolysis tests and TPO tests at different stages of the conditioning process led to conclude that the surface of the fresh catalyst is rich of defects, like steps and kinks, extremely active in C-forming reactions (e.g. C–H bond breaking). This extra-activity of the fresh surface would actually favour C-accumulation (especially between 500 and 650 °C), eventually contrasting the catalyst performance [1]. However, it was thought that the methodology of repeated runs at increasing temperature up to 850 °C promoted an enlargement of particles with gradual loss of defects and enhanced the reaching of a balance between C-forming and C-reforming reactions.

The present characterization results and the evidence of the different conditioning behaviour at varying preparation procedure confirm such picture. The low initial activity of the NT sample and the long duration of the conditioning process could be related with a certain ''resistance'' of the surface to the reconstruction (formation of more densely packed particles); indeed, HRTEM indicates that, after ageing, this sample had the smallest average particle size and kept a certain fraction of small rafts. Montini et al. [23] have reported a lower stability of a Rh/Al_2O_3 catalysts prepared by impregnation with respect to $Rh@Al_2O_3$ with embedded Rh particles and have explained the observation with a certain tendency of the traditional Rh-catalyst to coke formation, which, we believe, is an indirect evidence of the presence of highly active defect sites even under high temperature reaction conditions. The surface reconstruction and the stabilization of the catalytic performance were apparently easier in the case of CB sample, despite the apparently similarity with the NT sample according to different characterization technique.

The interpretation on the nature of conditioning is also confirmed by the evidence that the best initial performance were shown by the sample with the highest degree of organization of Rh particles.

5. Conclusions

The present study provides new pieces of evidence for comprehending the relationship between surface structure and syngas catalysis of highly dispersed supported Rh-catalysts. In the case of low Rh load, it was shown that the preparation technique affects the initial catalytic activity, but after a conditioning transient process, differently prepared catalysts reach similar catalytic performances.

The combined results of the pulse-chemisorption analyses, the CO-DRIFT spectra and HRTEM concur to indicate that the surface of the fresh Rh-catalysts are heterogeneous, since isolated Rh sites, small raft particles and bigger well formed three-dimensional truncated octahedrals coexist. The relative abundance of rafts and isolated species with respect to three-dimensional particles is strongly affected by the preparation procedure; it was minimized by a CVD technique, while it was high in the case of the grafting and impregnation techniques. However, the exposition of the catalyst samples to high temperature methane-CPO conditions induced a reconstruction of the surface, since the heterogeneity was largely eliminated and the reorganization of isolated atoms and the smaller aggregates into bigger metallic particles occurred. This ''smoothening'' effect of the high temperature reaction can explain the presence and extent of the conditioning process, when considering the negative impact of Rh defect sites on the syngas catalysis related to the promotion of C deposition.

Acknowledgement

Funding from MIUR-Rome is gratefully acknowledged.

References

[1] A. Beretta, T. Bruno, G. Groppi, I. Tavazzi, P. Forzatti, Appl. Catal. B: Environ. 70 (2007) 515.
[2] T. Bruno, A. Beretta, G. Groppi, M. Roderi, P. Forzatti, Catal. Today 89 (2005) 89.
[3] D. Wang, O. Dewaele, G. Froment, J. Mol. Catal. A: Chem. 136 (1998) 301.
[4] J. Wei, E. Iglesia, J. Catal. 224 (2004) 370.
[5] J. Wei, E. Iglesia, J. Catal. 225 (2004) 116.
[6] Z.-P. Liu, P. Hu, J. Am. Chem. Soc. 125 (2003) 1958.
[7] J. Rostrup-Nielsen, J.K. Norskov, Top. Catal. 40 (1–4) (2006) 45.
[8] E. Finocchio, G. Busca, P. Forzatti, G. Groppi, A. Beretta, Langmuir 23 (2007) 10419.
[9] D.J.C. Yates, L.L. Murrel, E.B. Prestige, J. Catal. 57 (1979) 41.
[10] D.J.C. Yates, J.H. Sinfelt, J. Catal. 8 (1967) 348.
[11] J.C. Vis, H.F.J. van't Blink, T. Huizinga, J. van Grondelle, R. Prins, J. Catal. 95 (1985) 333.
[12] B.J. Kip, F.B.M. Duivenvoorden, D.C. Koningsberger, R. Prins, J. Catal. 105 (1987) 26.
[13] K. Walter, O.V. Buyevskaya, D. Wolf, M. Baerns, Catal. Lett. 29 (1994) 261.
[14] D.A. Bulushev, G.F. Froment, J. Mol. Catal. A: Chem. 139 (1999) 63.
[15] Z. Tian, O. Dewaele, G.B. Marin, Catal. Lett. 57 (1999) 9.
[16] L. Basini, D. Sanfilippo, J. Catal. 157 (1995) 162.
[17] L. Basini, A. Guarinoni, A. Aragno, J. Catal. 190 (2000) 284.
[18] S. Bernal, J.J. Calvino, M.A. Cauqui, J.A. Pérez Omil, J.M. Pintado, J.M. Rodrìguez-Izquierdo, Appl. Catal. B: Environ. 16 (1998) 127.
[19] S. Bernal, F.J. Botana, J.J. Calvino, G.A. Cifredo, J.A. Pérez-Omil, J.M. Pintado, Catal. Today 23 (1995) 219.

[20] J.M. Gatica, R.T. Baker, P. Fornasiero, S. Bernal, G. Blanco, J. Kaspar, J. Phys. Chem. B 104 (2000) 4667.
[21] G. Vlaic, P. Fornasiero, G. Martora, E. Fonda, J. Kaspar, L. Marchese, E. Tomat, S. Cosuccia, M. Graziani, J. Catal. 190 (2000) 182.
[22] A. Maroto-Valiente, I. Rodrìguez-Ramos, A. Guerriero-Ruiz, Catal. Today 93 (2004) 567.
[23] T. Montini, A.M. Condò, N. Hickey, F.C. Lovey, L. De Rogatis, P. Fornasiero, M. Graziani, Appl. Catal. B: Environ. 73 (2007) 84.
[24] L. Basini, M. Marchionna, A. Aragno, J. Phys. Chem. 96 (1992) 9431.
[25] V. Dal Santo, A. Beretta, V. De Grandi, A. Gallo, R. Psaro, L. Sordelli, S. Recchia, Nanosmat 2007, 2nd International Conference on Surfaces, Coatings and Nanostructured Materials, July 9–11, 2007, Alvor, Algarve, Portugal, Book of Abstract, p. 134.
[26] W. Ibashi, G. Groppi, P. Forzatti, Catal. Today 83 (2003) 115.
[27] I. Tavazzi, A. Beretta, G. Groppi, P. Forzatti, J. Catal. 241 (2006) 1–13.
[28] C. Wong, R.W. McCabe, J. Catal. 119 (1989) 47.
[29] P.G. Menon, J. Sieders, F. Streefkerk, G.J.M. van Keulen, J. Catal. 29 (1973) 188.
[30] J.E. Benson, M. Boudart, J. Catal. 4 (1965) 704.
[31] S.E. Wanke, N.A. Dougharty, J. Catal. 24 (1972) 367.
[32] V. Dal Santo, C. Dossi, A. Fusi, R. Psaro, C. Mondelli, S. Recchia, Talanta 66/3 (2005) 674.
[33] P.B. Rasband, W.C. Hecker, J. Catal. 139 (1993) 551.
[34] K.I. Hadjiivanov, G.N. Vayssilov, Adv. Catal. 47 (2002) 308.
[35] D.K. Paul, C.D. Marten, J.T. Yates Jr., Langmuir 15 (1999) 4508.
[36] J.T. Yates Jr., T.M. Duncan, R.W. Vaughan, J. Chem. Phys. 71 (1979) 3908.
[37] I.M. Hamadeh, P.R. Griffiths, Appl. Spectrosc. 41 (1987) 682.
[38] I.A. Fischer, A.T. Bell, J. Catal. 162 (1996) 54.
[39] J. Kaspar, C. de Leitenburg, P. Fornasiero, A. Trovarelli, M. Graziani, J. Catal. 146 (1994) 136.
[40] L.L. Sheu, W.M.H. Sachtler, J. Mol. Catal. 81 (1993) 267–278.
[41] P. Basu, D. Panayotov, J.T. Yates Jr., J. Phys. Chem. 91 (1987) 3133.
[42] G.A. Somorjai, Surf. Sci. 335 (1995) 10.
[43] N. Kruse, A. Gaussman, J. Catal. 144 (1993) 525.
[44] C. Voss, N. Kruse, Surf. Sci. 409 (1998) 252.
[45] K.K. Bando, N. Ichikuni, K. Soga, K. Kunimori, H. Arakawa, K. Asakura, J. Catal. 194 (2000) 91.
[46] J.D. Grunwaldt, L. Basini, B.S. Clausen, J. Catal. 200 (2001) 321.
[47] F. Cimini, R. Prins, J. Phys. Chem. B 101 (1997) 5285.
[48] R. Schennach, G. Krenn, B. Klotzer, K.D. Rendulic, Surf. Sci. 540 (2003) 237.
[49] R. Horn, K.A. Williams, N.J. Degenstein, A. Bitsch-Larsen, D. Dalle Nogare, S.A. Tupy, L.D. Schmidt, J. Catal. 249 (2) (2007) 380.